

Elevated *O*-GlcNAc-dependent signaling through inducible mOGT expression selectively triggers apoptosis

Sang-Hoon Shin · Dona C. Love · John A. Hanover

Received: 5 April 2010 / Accepted: 3 August 2010 / Published online: 8 September 2010
© The Author(s) 2010. This article is published with open access at Springerlink.com

Abstract *O*-linked *N*-acetylglucosamine transferase (OGT) catalyzes *O*-GlcNAc addition to numerous cellular proteins including transcription and nuclear pore complexes and plays a key role in cellular signaling. One differentially spliced isoform of OGT is normally targeted to mitochondria (mOGT) but is quite cytotoxic when expressed in cells compared with the ncOGT isoform. To understand the basis of this selective cytotoxicity, we constructed a fully functional ecdysone-inducible GFP–OGT. Elevated GFP–OGT expression induced a dramatic increase in intracellular *O*-GlcNAcylated proteins. Furthermore, enhanced OGT expression efficiently triggered programmed cell death. Apoptosis was dependent upon the unique N-terminus of mOGT, and its catalytic activity. Induction of mOGT expression triggered programmed cell death in every cell type tested including INS-1, an insulin-secreting cell line. These studies suggest that deregulated activity of the mitochondrially targeted mOGT may play a role in triggering the programmed cell death observed with diseases such as diabetes mellitus and neurodegeneration.

Keywords *O*-GlcNAc · *O*-linked *N*-acetylglucosamine transferase · Apoptosis

Introduction

O-linked *N*-acetylglucosamine (*O*-linked GlcNAc) attachment to Ser/Thr residues of proteins has been termed *O*-GlcNAcylation. *O*-linked-*N*-acetylglucosamine transferase (OGT) catalyzes this reversible glycan modification of nuclear and cytoplasmic proteins. A neutral hexosaminidase *O*-GlcNAcase removes *O*-GlcNAc [For reviews see (Butkinaree et al. 2010; Hanover et al. 2010; Lazarus et al. 2009a; Love and Hanover 2005; Hart et al. 2007; Wells et al. 2001)]. Despite recent advances in defining the enzymes of *O*-GlcNAc metabolism, the cellular function of *O*-GlcNAcylation of proteins is poorly understood. *O*-GlcNAcylated proteins include oncogenes, tumor suppressors, kinases, nuclear pore proteins, transcription factors, nuclear hormone receptors, and RNA polymerase II itself (Butkinaree et al. 2010; Hanover et al. 2010; Love and Hanover 2005; Slawson et al. 2006). Clearly OGT plays essential functions in the regulation of transcription (Gambetta et al. 2009; Sinclair et al. 2009; Love et al. 2010). Genetic analysis in *C. elegans* also links *O*-GlcNAc directly to cell signaling (Forsythe et al. 2006; Hanover et al. 2005; Love et al. 2010). Other cellular proteins such as the cytokeratins, tau, clathrin assembly protein AP3, and the amyloid precursor protein (APP) are also *O*-GlcNAcylated (Butkinaree et al. 2010; Hanover et al. 2010; Love and Hanover 2005; Slawson et al. 2006). It has been suggested that reversible modification by *O*-GlcNAc may act in parallel with protein phosphorylation to modify protein–protein interactions (Butkinaree et al. 2010). *O*-GlcNAc may also stabilize proteins by preventing degradation. Given the large number of substrates modified by *O*-GlcNAc, such modification may perform many cellular functions (Hanover 2001; Butkinaree et al. 2010; Hanover et al. 2010; Lazarus et al. 2009a; Love and Hanover 2005; Hart et al. 2007; Wells et al. 2001).

D. C. Love · J. A. Hanover (✉)
Laboratory of Cell Biochemistry and Biology,
NIDDK, National Institutes of Health,
Bldg 8 Rm B127, 8 Center Dr MSC 0850,
NIH, Bethesda, MD 20892-0850, USA
e-mail: jah@helix.nih.gov
URL: <http://www.niddk.nih.gov/intram/people/jhanover.htm>;
http://intramural.niddk.nih.gov/research/PIResearch.asp?People_ID=1608&Title=Current%20Research:

S.-H. Shin
Gyeong-Gi Bio Center, Suwon, Korea

A number of findings strongly suggest that OGT may perform a signaling function. *O*-linked GlcNAc transferase is well conserved across species. The higher plant *Arabidopsis* has a homolog termed *Spindly* involved in the gibberellin-dependent signaling pathway. Mutations in *Spindly* cause constitutive activation of gibberellin signaling (Banerjee et al. 2009; Chen et al. 2005; Filardo et al. 2009; Hartweck et al. 2006; Hartweck et al. 2002; Robertson et al. 1998; Silverstone et al. 2007). In mammals, OGT is located in the X chromosome and is essential for stem cell survival and embryonic development in mouse (Shafi et al. 2000; Hanover et al. 2003). The OGT gene is alternatively spliced to produce a number of differentially targeted isoforms with variable amino termini (Hanover et al. 2003; Love et al. 2003). The two main isoforms are targeted to the nucleus and cytoplasm (ncOGT) and the mitochondrion (mOGT) (Hanover et al. 2003; Love et al. 2003). After the variable amino terminus, OGT isoforms contain 2–12 tetratricopeptide repeats (TPR), 34 amino acid repeat motifs thought to mediate protein–protein interactions. The TPR motif is found in proteins regulating cell cycle control, transcription repression, stress response, as well as mitochondrial and peroxisomal protein transport (Butkinaree et al. 2010; Hanover et al. 2010; Lazarus et al. 2009a; Slawson et al. 2006). OGT isoforms may also contain a nuclear localization signal and a catalytic domain with similarities to glycogen phosphorylase and certain glycosyltransferases (Kreppel and Hart 1999; Lubas and Hanover 2000; Roos and Hanover 2000). OGT transcripts are also enriched in pancreatic beta cells (Hanover et al. 1999). These molecular features suggested that OGT isoforms might play a role in glucose sensing and diabetes mellitus (Lubas et al. 1997). OGT may also play a role in other human diseases. Streptozotocin (STZ), an analog of GlcNAc, is a beta cell toxin and has been shown to inhibit *O*-GlcNAcase (Roos et al. 1998; Hanover et al. 1999) and the resulting elevation of *O*-GlcNAc levels have been suggested to be part of the mechanism of selective beta cell death (Liu et al. 2000). A growing body of evidence now suggests that *O*-GlcNAcylation plays a key role in the development of insulin resistance, the signature of type 2 diabetes (McClain et al. 2002; Vosseller et al. 2002).

Insulin resistance leads to the gradual loss of Beta cell function and overt diabetes (Liu et al. 2000; Olefsky 2001). The hexosamine biosynthetic pathway has long been implicated in insulin resistance (Marshall et al. 1991). A small percentage of glucose entering cells is converted to UDP-GlcNAc via a pathway involving the rate-limiting enzyme glutamine fructose 6-phosphate amido transferase (GFAT) (Brownlee 2001; Butkinaree et al. 2010; Hanover et al. 2010; Lazarus et al. 2009b; Love and Hanover 2005;

Slawson et al. 2006). UDP-GlcNAc feedback inhibits the activity of GFAT (Kornfeld 1967). UDP-GlcNAc then serves as the donor for OGT (Butkinaree et al. 2010; Hanover et al. 2010; Lazarus et al. 2009a; Love and Hanover 2005). We demonstrated that OGT mediates the effects of the hexosamine biosynthetic pathway in generating insulin resistance (McClain et al. 2002). Other lines of evidence suggest that OGT may play a role in neurodegenerative diseases (Butkinaree et al. 2010; Hanover 2001; Hanover et al. 2010; Hart et al. 2007; Lazarus et al. 2009b; Liu et al. 2004; Love and Hanover 2005; Nakamura et al. 2001). Human OGT is located on Xq13 where it was previously mapped as a candidate region for Lubag syndrome or X-linked dystonia-parkinsonism. Hyperphosphorylated forms of Tau are associated with neurofibrillary tangles in Alzheimer's disease, while it is modified by *O*-GlcNAcylation in normal brain. Other neuronal proteins such as Ankyrin, neurofilaments, synapsin, and MAP1 are also modified by *O*-GlcNAc (Butkinaree et al. 2010; Hanover 2001; Hanover et al. 2010; Hart et al. 2007; Lazarus et al. 2009b; Liu et al. 2004; Love and Hanover 2005; Nakamura et al. 2001).

O-linked GlcNAc transferase (OGT) has been suggested to mediate a novel glycan-dependent signal transduction pathway (Butkinaree et al. 2010; Hanover et al. 2005, 2010; Love and Hanover 2005; Slawson et al. 2006; Forsythe et al. 2006). The isoforms of OGT show interesting differences in their toxicity upon overexpression. The ncOGT isoform is largely non-toxic upon overexpression while mOGT overexpression is cytotoxic (Hanover et al. 2003; Lubas et al. 1997; Love et al. 2003).

In this paper, we describe an inducible expression system for OGT where either isoform can be expressed. Our results suggest that mOGT overexpression enhances *O*-GlcNAcylation and induces apoptosis. We show that OGT-dependent apoptosis requires OGT catalytic activity and occurs in multiple cells including an insulinoma cell line, INS-1. Programmed cell death is an essential mechanism for regulating cell number and cell fate. Our findings suggest a role of *O*-GlcNAc signaling in the induction of apoptosis. This may have important implications for the programmed cell death associated with hexosamine metabolism such as diabetes mellitus and neurodegeneration.

Materials and methods

DNA constructions

Ecdysone-inducible, GFP-fused OGT vector, pIND/GFP-OGT, was generated by ligating the *Nhe*I and *Not*I digested

fragment of CMV-driven pGFP-OGT (Love et al. 2003) into pIND vector with the neomycin selection marker (Invitrogen, Carlsbad, CA, USA). The orientation of this construct is mOGT followed by GFP. C-terminal truncated OGT, without catalytic activity, pGFP-OGT-G, was generated by ligating the XhoI digestion fragment of pGFP-OGT into the pEGFPC2 (Invitrogen) (Lubas and Hanover 2000). pI-mOGT-G-IRES-GFP, pI-4A-mOGT-IRES-GFP, and pI-4A-mOGT-G-IRES-GFP were derived from the pI-mOGT-IRES-GFP construct created as described above for pIND/GFP-OGT but using an mOGT-IRES-GFP cassette.

Tissue culture, transfection, and isolation of a stable cell line expressing GFP-OGT

Human embryonic kidney fibroblast cell line EcR-293 (Invitrogen) (ATCC, CRL-1573) stably expresses the functional ecdysone receptor. EcR-293 cells were grown on six-well dishes in Dulbecco's Modified Eagle Medium (high glucose), 10% Fetal Bovine Serum, 2 mM L-glutamine, 1% Pen/Strep, and 400 µg/ml of Zeocin. Insulin-secreting cell line, INS-1, was maintained as described earlier (Asfari et al. 1992). 1 µg of DNA was used for the transfection with FuGENE 6 (Roche) according to the manufacturer's instructions. Stable cell lines were selected in the presence of 800 µg/ml of G418 and positive green fluorescent cell lines were isolated using cloning cylinders 20 h after the induction with Ponasterone A. For induction, media were changed after 23-h transfection with FuGENE6, and ecdysone homolog Ponasterone A (Invitrogen) was added into fresh media and incubated for another 20 h before the observation of induced expression of GFP fused proteins.

Immunoblot analysis

After induction with the ecdysone homolog Ponasterone A, cells were lysed in the presence of 10 mM leupeptin, 10 mg/ml aprotinin, and 17.4 mg/ml PMSF and boiled for 1 min at 98°C before loading. The proteins were resolved using 4–12% Tris-Glycine buffered SDS/PAGE analysis. Separated proteins were transferred onto nitrocellulose and induced GFP-OGT was detected by using 1:200 diluted GFP peptide antibody (CLONTECH), followed by 1:4,000 diluted horseradish peroxidase (HRP)-conjugated goat anti-rabbit antibody (Jackson ImmunoResearch). *O*-linked *N*-acetylglucosaminylated proteins were detected by using the diluted RL2 mouse monoclonal IgG1 (1:5,000) antibody (Affinity BioReagents), followed by 1:1,000 diluted HRP-conjugated anti-mouse antibody. Enhanced chemiluminescence (ECL) detection method (Amersham) was used to develop images.

Immunocytochemistry

Cells were grown on the coverslips for 24 h. After washing with phosphate-buffered saline (PBS), cells were incubated with 4% formaldehyde for 30 min. Formaldehyde-fixed cells were washed twice with PBS and then permeabilized with 0.2% Triton X-100 for 2 min. Cells were rinsed with PBS four times over 5 min. In a humidified chamber, cells were incubated with 1:100 diluted RL2 in 3% bovine serum albumin (BSA) for 45 min. After washing with PBS, cells were incubated with 1:100 diluted FITC-conjugated anti-mouse antibody for 20 min.

Fluorescence and light microscopy

Fluorescence images were taken using an Axiovert 100 TV (Zeiss) with IPLab scientific imaging software (Scanalytics) or LSM410 confocal microscope (Zeiss) with its Zeiss LSM 410 software. Optical images from TUNEL assays were obtained with Hamamatsu C5810 color chilled 3CCD camera (Hamamatsu).

TUNEL (terminal deoxynucleotidyl transferase-mediated dUTP nick translation) assay

Programmed cell death (apoptosis) was detected immunohistochemically using horseradish peroxidase (HRP) according to the manufacturer's instructions as described below (Roche). Cells were fixed with freshly made 4% paraformaldehyde for 1 h. Cells were rinsed with PBS between each step. To block endogenous peroxidase, cells were incubated with 3% hydrogen peroxide in methanol for 10 min. Cells were permeabilized with 0.1% Triton X-100 in 0.1% sodium citrate for 2 min at 4°C. Bovine pancreatic deoxyribonuclease I (Boeringer Mannheim) was used to cleave DNA for the positive control of the assay. Terminal deoxynucleotidyl transferase (TdT) from calf thymus was added to the cells in a fluorescein-labeled nucleotide mixture reaction buffer for 1 h at 37°C. HRP-conjugated anti-fluorescein antibody was added to incubate cells for 30 min at 37°C. Cells were incubated with DAB substrate for 10 min followed by light microscopy.

Annexin V apoptosis assay

Annexin V-Biotin Apoptosis detection kit (ALEXIS Biochemicals) was used according to the manufacturer's instructions as described below. Cells on the coverslips were rinsed with PBS twice. Cells were incubated with 5 µl of Annexin V-Biotin and 200 µl of 1× binding buffer for 5 min in the dark. Cells were washed once in 200 µl of 1× binding buffer. Cells were fixed with 2% formaldehyde for 15 min and resuspended with 100 µl of 0.1% BSA in PBS.

5 $\mu\text{g/ml}$ of streptavidin–rhodamine was added and incubated for 15 min followed by fluorescence microscopy. Camptothecin (3 $\mu\text{g/ml}$) was used to induce apoptosis for the positive control of apoptosis.

DNA ladder apoptosis assay

ApoAlert LM-PCR ladder assay kit (CLONTECH) was used following the manufacturer's instructions as summarized below. Genomic DNA was mixed with adapter DNA in ligation mix and heated to 55°C for 10 min and allowed to cool to 10°C over 1 h. T4 ligase was added to the tube and incubated at 16°C overnight. PCR reaction of adaptor-ligated DNA was incubated for 3 min at 72°C and then added to Advantage cDNA Polymerase mix and amplified according to manufacturer's instructions (CLONTECH). Calf thymus DNA was used for the positive control. Nucleosomal ladder appears as multiples of approximate 200 bp.

Results

Previously, we showed that transient overexpression of the mitochondrial form of OGT (mOGT) increased cellular

OGT activity, but was cytotoxic (Hanover et al. 2003; Lubas et al. 1997). Overexpression of the ncOGT isoform did not show obvious cytotoxicity. To understand the basis for the selective cytotoxicity, we have developed a conditional expression system of OGT in mammalian cell lines. We used an ecdysone-inducible gene expression system (outlined in Fig. 1). To identify the subtle difference of OGT expression in the cells, we first added the green fluorescence protein (GFP) as a second marker and an internal ribosomal entry site (IRES). When this construct was transfected into cells, in the presence of the ecdysone analog ponasterone A, the ecdysone-dependent inducible promoter directed the production of a bicistronic transcript encoding two proteins: mOGT and GFP, which is translated independently using the IRES. We observed colonies from stably transfected cells under selective pressure of G418 in the absence of ponasterone A. We could not generate a stable cell line from the dishes transfected with pI-mOGT-IRES-GFP. However, we got stable cell lines stably expressing the inactive pI-mOGT-G-IRES-GFP, containing C-terminal deletion. Interestingly, we observed an order of magnitude higher number of colonies derived from either pI-4A-mOGT-IRES-GFP (containing a N-terminal deletion) or pI-4A-mOGT-G-IRES-GFP (containing both N- and C-terminal deletions) (Fig. 1) in comparison with the dishes

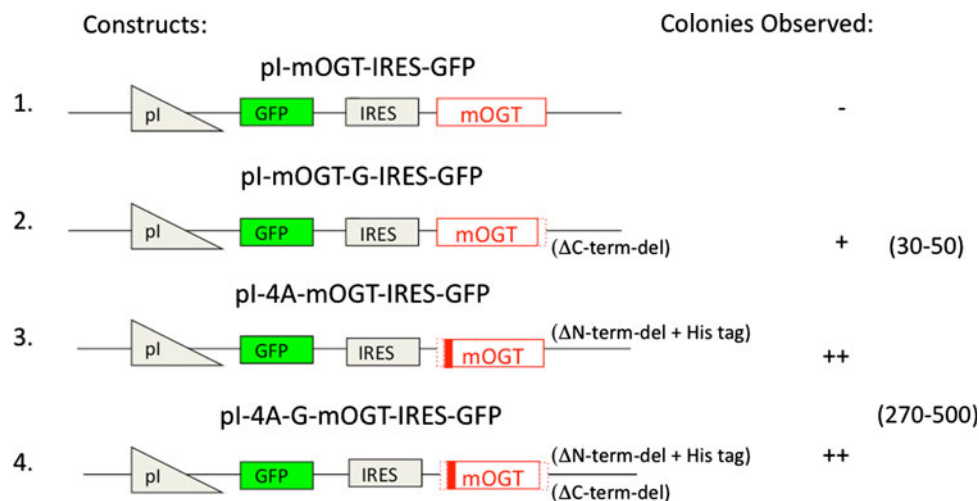


Fig. 1 Inducible expression of mOGT in IRES bicistronic vectors leads to toxicity requiring proper targeting and catalytic activity. 1. pI-mOGT-IRES-GFP has the full length OGT gene placed after an ecdysone-inducible promoter and an internal ribosomal entry site is located between OGT and GFP. This vector is used as a backbone for the derivatives described below. 2. pI-mOGT-G-IRES-GFP contains a C-terminal deletion represented by *dotted lines* ($\Delta\text{C-term-del}$). This catalytically defective mOGT replaces the full length wild-type mOGT. 3. pI-mOGT-4A-IRES-GFP contains a deletion (*dotted lines*) of the 15 N-terminal amino acids thought to be involved in mitochondrial targeting (MLQGHFWLREGIMIS) and has an added

histidine tag (*solid red stripe*) at the N-terminus ($\Delta\text{N-term-del} + \text{His tag}$). 4. pI-mOGT-4A-G-IRES-GFP is catalytically defective and contains both C-terminal and N-terminal deletions plus the histidine tag described for vectors 2 and 3, respectively. These plasmids were transfected into EcR-293 cells and the surviving colonies were selected with G418 as described. Colonies were counted to quantify the degree of toxicity for each construct. The minus sign means no colonies were observed. There is roughly an order of magnitude difference between one plus and two plus signs. Approximate colony numbers are shown. The colony count was carried out in triplicate and a summary of the three experiments is presented

transfected with pI-mOGT-G-IRES-GFP. With bicistronic constructs, we saw a minimal level of transient or stable expression of either mOGT or GFP in the absence of ponasterone A. These experiments suggested that upon removal of the 15 amino acid N-terminus of mOGT (pI-4A-mOGT-IRES-GFP), or by inactivating the catalytic domain of mOGT by truncation (pI-mOGT-G-IRES-GFP), much of the toxicity of mOGT was eliminated.

In another series of experiments, GFP was directly appended to the amino terminus of the 103-kDa isoform of mOGT and placed under the control of the ecdysone promoter, pIND/GFP-OGT (Fig. 2a). This allowed direct visualization and detection of the mOGT transgene. Expression of this fusion protein was monitored by

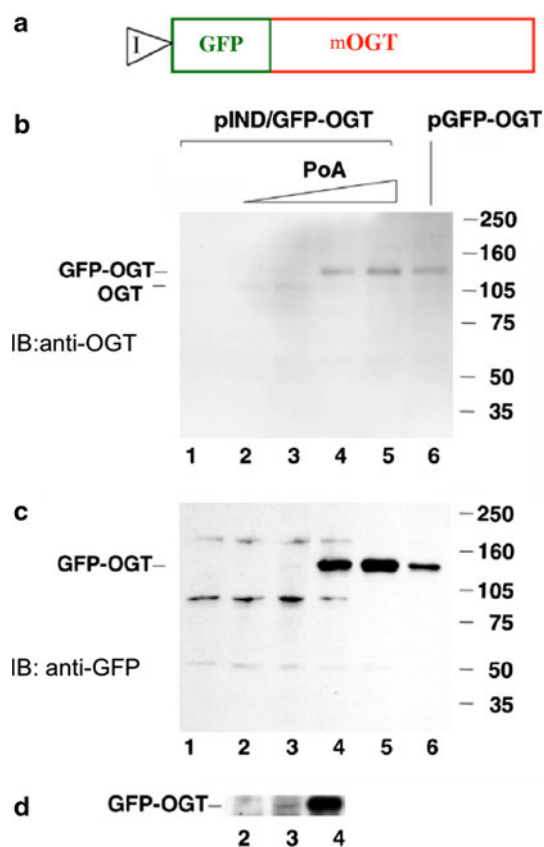


Fig. 2 Inducible expression of mOGT in EcR293 cells. **a** Diagram of the GFP-mOGT construct under the control of an inducible promoter (pIND/GFP-OGT). **b** Western blot analysis using an anti-OGT antibody to compare expression levels of pIND/GFP-OGT with increasing amounts of Ponasterone A (PoA) to a CMV-driven GFP-OGT fusion (pGFP-OGT). **c** Western blot analysis of same samples using an anti-GFP antibody. For **b** and **c** EcR-293 cells were transfected with pIND/GFP-OGT and incubated without Ponasterone A (PoA) (lane 1), or with the following concentration of PoA: 0.1 μM (lane 2), 0.5 μM (lane 3), 3.0 μM (lane 4), 15.0 μM (lane 5). Cells were also transfected with the CMV-driven plasmid pGFP-OGT (lane 6). On the right side are molecular weight markers. **d** Longer exposure of the Western blot shown in **c** between lanes 2 and 4 at 140 kDa range

immunoblotting (Fig. 2b–d). Increasing concentrations of Ponasterone A induced expression of the fusion protein. This expression was detected by an anti-OGT antibody (Fig. 2b) or an anti-GFP antibody (Fig. 2c, d). The level of expression observed when fully induced compared favorably with that seen using a CMV promoter, pGFP-OGT (Fig. 2b, c; compare lanes 5 and 6). Longer exposures of the immunoblots revealed that even at low levels of Ponasterone A, induction of OGT occurred (Fig. 2d). These data suggest that the ecdysone system allowed exquisite control over the levels of OGT expression.

To confirm that the GFP-OGT fusion protein was catalytically active, the levels of *O*-GlcNAc were examined using anti-*O*-GlcNAc antibodies and immunoblotting and immunofluorescence microscopy (Fig. 3). Increasing concentrations of Ponasterone A lead to increased *O*-GlcNAc levels on several cellular proteins (Fig. 3a). By immunofluorescence, we observed a substantial increase in *O*-GlcNAc in those cells induced to express the GFP-OGT fusion protein; no elevation was observed in those cells not expressing the fusion protein (Fig. 3b, pIND/GFP-OGT). Similar results were observed when a constitutive CMV promoter (pGFP-OGT) was used (Fig. 3b, pGFP-OGT). When we expressed a GFP-OGT fusion with a truncation in the catalytic domain, which renders it inactive (Lubas and Hanover 2000), *O*-GlcNAc levels were not elevated (Fig. 3b, pGFP-OGT-G). These data suggest that GFP-OGT is catalytically active when expressed in cells; this activity requires an intact OGT catalytic domain.

We then examined the effects of elevated *O*-GlcNAc levels on cell viability. The cell line EcR-293 (a kidney line) was chosen because it contains low levels of OGT (Lubas et al. 1997; Kreppel et al. 1997) and stably expresses ecdysone receptor which facilitates the ecdysone induction. Transient overexpression of catalytically active OGT was found to induce apoptosis as measured by the TUNEL assay (Fig. 4a, pGFP-OGT). The apoptosis was dependent upon catalytic activity since the transfection with the C-terminus deleted, catalytically defective, mutation of OGT did not result in TUNEL-positive cells (Fig. 4b, pGFP-OGT-G).

We generated an EcR-293 cell line expressing ecdysone-inducible GFP-OGT (pIND/GFP-OGT) and examined the response of these cells to increasing concentrations of Ponasterone A (Fig. 4e–g). The TUNEL-positive cells increased in number and intensity in response to hormone treatment. Treatment of 293 cells that did not express GFP-OGT with high levels of Ponasterone A (Fig. 4h, no plasmid) did not induce apoptosis. We have also confirmed these findings using an Annexin V assay (Fig. 4i–l). Cells expressing GFP-OGT (Fig. 4i) were positive (Fig. 4j) for Annexin V. Cells not expressing GFP-OGT were Annexin V negative (Fig. 4k). The apoptosis inducing drug, camptothecin, rendered all cells Annexin V-positive (Fig. 4l).

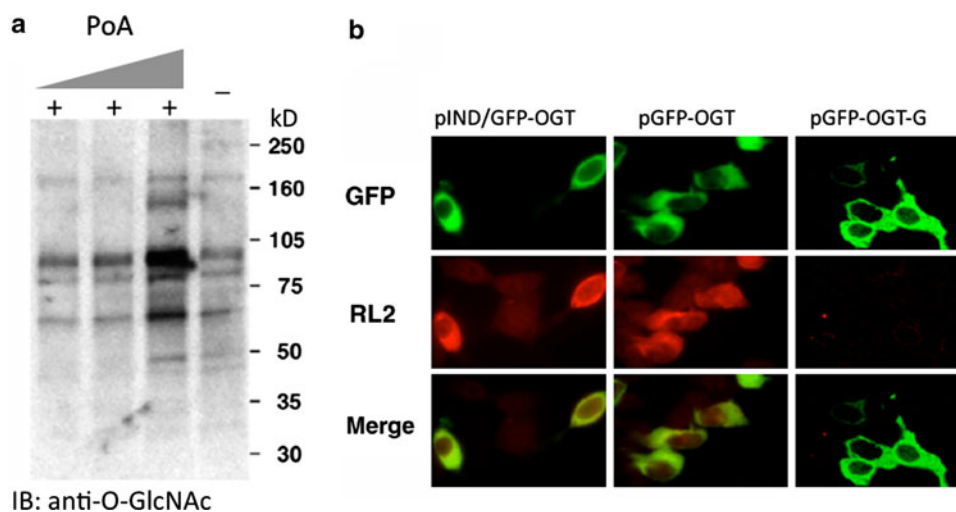


Fig. 3 *O*-GlcNAcylation is consistent with GFP-fused OGT expression, but not with mutant, catalytically defective, OGT. **a** Western blot analysis reveals that induction of GFP-fused OGT expression with increasing concentrations of Ponasterone A (PoA) (0.5, 3, 15 μM , respectively) causes an increase in the levels of total *O*-GlcNAc modification. The level of *O*-GlcNAc modified proteins

prior to induction is shown in the *last lane* (-). The anti-*O*-GlcNAc antibody, RL2, was used in the Western Blot analysis. **b** Immunofluorescent detection of GFP-fused OGT expression and its catalytic activity using RL2 staining. RL2 specifically recognizes *O*-GlcNAcylated proteins. pGFP-OGT-G is the c-terminal deleted, catalytically defective OGT under CMV-driven promoter

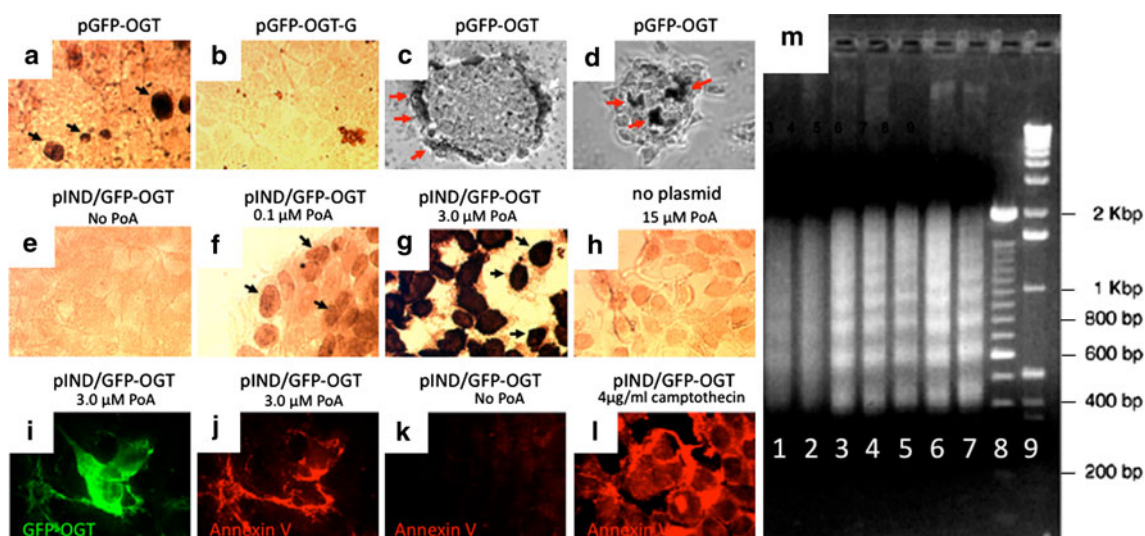


Fig. 4 Overexpression of catalytically active GFP-OGT induces apoptosis. **a** CMV-driven expression of the mitochondrial form of OGT (pGFP-OGT) induces apoptosis as shown by the TUNEL assay. **b** A catalytically inactive form of OGT (pGFP-OGT-G) does not induce apoptosis. ECR-293 cells were used for transfections in **a** and **b**. **c** and **d** An insulinoma cell line, INS-1, was transfected with active OGT (pGFP-OGT). The TUNEL assay was used to reveal apoptotic cells. Representative focal planes near the *bottom* (**c**) and *top* (**d**) of INS-1 cell clusters are shown. Note the apoptotic cells on the outer layer of cells in the clusters. *Black* and *red* arrows denote cells scored as positive by the TUNEL assay. **e-g** ECR-293 cells were transfected with GFP-OGT (pIND/GFP-OGT) and induced with Ponasterone A (PoA) at indicated concentrations. Note the increasing amount of TUNEL-positive cells (*black* arrows) in **g** and **h** compared with the two negative controls **e** and **h** pIND/GFP-OGT, no PoA and no plasmid, 15 μM PoA, respectively. **i-l** Annexin V staining was used

to identify apoptotic cells. **i** ECR-293 cells were treated with 3.0 μM of Ponasterone A to induce expression of pIND/GFP-OGT (*green*). **j** Same field stained with an anti-annexin V antibody to reveal apoptotic cells (*red*). Note near-complete colocalization of GFP-OGT expression and Annexin V staining (compare **i** and **j**). **k** Untreated cells did not stain positive for Annexin V. **l** As a positive control for apoptosis, 4 $\mu\text{g/ml}$ camptothecin was added to uninduced cells. **m** DNA ladder assay. Genomic DNA from pIND/GFP-OGT transfected cells (*lanes 1-5*) was separated on an agarose gel to reveal DNA laddering. Uninduced cells are shown in *lane 1*. Increasing amounts of Ponasterone A were added at the following concentrations: 0.1 μM (*lane 2*), 0.5 μM (*lane 3*), 3.0 μM (*lane 4*), 15.0 (*lane 5*). The DNA laddering from CMV-driven expression of pGFP-OGT (*lane 6*) is comparable to the commercially available positive control from Calf thymus (lane 7). DNA size markers of 100 bp (*lane 8*) and 1 kb DNA (*lane 9*) are shown

Final confirmation that GFP-OGT induces apoptosis was obtained by a DNA ladder assay (Fig. 4m). Increasing concentrations of ecdysone (Lanes 2–5) caused DNA laddering, identical to that seen in a positive control (Lane 7). Similar results were obtained using unmodified mOGT under the control of the CMV promoter (Lane 6). Taken together, these findings strongly suggest that elevation in the levels of cellular mOGT induces apoptosis in EcR-293 cells. We were interested in seeing whether the apoptotic effect observed with elevated OGT expression was restricted to kidney fibroblast-derived EcR-293 cells. We chose to examine the effects of elevated OGT expression in the insulinoma-derived INS-1 cell line since this cell line has many similarities to pancreatic beta cells. Many TUNEL-positive apoptotic cells were found in INS-1 cells following transfection with the mOGT (Fig. 4c, d). OGT-induced apoptosis was also observed in HeLa cells and CHO cells (data not shown). Thus, triggering of apoptosis appears to be a general cellular response to elevated mOGT expression.

Discussion

Our findings regarding elevated mOGT expression and the triggering of apoptosis are intriguing in light of more recent findings linking the hexosamine biosynthetic pathway with other signaling pathways including those involved in programmed cell death and mitochondrial function. The role of the hexosamine biosynthetic pathway in insulin signaling is well documented. First, we have shown that overexpression of OGT in muscle and fat of transgenic mice induces insulin resistance (McClain et al. 2002). Similar conclusions were reached in L1-3T3 cells using an inhibitor of *O*-GlcNAc removal to elevate *O*-GlcNAc levels (Vosseller et al. 2002). These effects appear to be linked to alteration of the AKT-signaling pathway. This kinase is associated with numerous signaling pathways including the insulin-signaling pathway and the pathways controlling apoptosis (Butkinaree et al. 2010; Hanover et al. 2010; Lazarus et al. 2009a; Slawson et al. 2006). We have shown that several kinases associated with this cascade, including casein kinase II and GSK3 β are substrates for OGT (Lubas and Hanover 2000; Lazarus et al. 2006). In addition, *O*-GlcNAc is associated with beta cell destruction in a process involving apoptosis (Liu et al. 2000). Glucosamine administration has been shown to induce programmed cell death in tissue culture (Liu et al. 2000; Tang et al. 2000). Glucosamine also blocks the neuroprotective effect of insulin and induces apoptosis in retinal neurons (Nakamura et al. 2001). *O*-GlcNAc levels must be tightly controlled in cardiac tissue (Champattanachai et al. 2007; Champattanachai et al. 2008; Fulop et al. 2007; Laczy et al. 2009; Wu

et al. 2009). Increased *O*-GlcNAcylation of mitochondrial proteins impairs mitochondrial function in cardiac myocytes exposed to high glucose (Hu et al. 2009). On the other hand, glucosamine protects neonatal cardiomyocytes from injury via increased Bcl-2 and *O*-GlcNAc (Champattanachai et al. 2008).

More direct evidence that hexosamine synthesis is involved in apoptotic signaling derives from studies of MEFs deficient in glucosamine-6-phosphate (GlcN6P) acetyltransferase (EMeg32). These fibroblasts produce very low levels of UDP-GlcNAc (Boehmelt et al. 2000) and lower levels of *O*-GlcNAc modified cytosolic and nuclear proteins while other pathways are unaffected. Interestingly, growth-impaired EMEg32 (–/–) MEFs withstand a number of apoptotic stimuli and express activated PKB/AKT. These findings strongly suggest that UDP-GlcNAc levels influence cell cycle progression and susceptibility to apoptotic stimuli. By utilizing UDP-GlcNAc to modify cellular proteins, OGT may induce apoptosis in response to elevated flux through the hexosamine signaling pathway. In addition to our current findings, the most direct evidence for a role of OGT in apoptotic signaling derives from a screen of anti-apoptotic genes in leukemia cells (Fletcher et al. 2002). In parallel with our studies on OGT isoforms, a functional retroviral cDNA library-based screen was employed to identify genes that prevent growth factor withdrawal-mediated apoptosis in a myeloid progenitor cell. This approach identified a truncated form of OGT as an anti-apoptotic factor (Fletcher et al. 2002). Based on the properties of the protein, these authors argued that the truncated form of OGT identified was functioning as a dominant negative inhibitor of OGT. The coding sequence of OGT identified by Fletcher et al. (2002), corresponds to a form of OGT we have referred to as sOGT (Hanover et al. 2003; Love et al. 2003), a short splice variant of approximately 78 kDa derived from the OGT gene. This OGT isoform has nearly two complete and one partial TPR motifs. It is substantially shorter than the 103-kDa mOGT isoform used in this study, but contains the intact catalytic domain of OGT. Many apoptotic-signaling molecules such as bax have a corresponding family member that is anti-apoptotic (such as bcl-2, bcl-x or mcl-1). These observations raise the possibility that mOGT and sOGT represent pro- and anti-apoptotic partners involved in regulating apoptosis. Their balance may be essential for regulating programmed cell death. These studies also suggest a mechanism by which elevated flux through the hexosamine-signaling pathway may be linked to apoptosis. The programmed cell death may have relevance for Beta cell loss in diabetes mellitus, and numerous other human diseases undergoing apoptosis.

We note, with great interest, that the ncOGT interacts with Ataxin-10 in the brain and pancreas and that the sOGT

variant interferes with this interaction (Andrali et al. 2005; Marz et al. 2006). These findings and the findings outlined above suggest that each of the isoforms of OGT may be key regulators of pro-survival mechanisms in the nucleus, cytoplasm and mitochondrion. Further work will be required to thoroughly understand the significance of these many interactions.

Acknowledgments We thank Wendy Wu, Bill Lubas for their contributions and stimulating discussions and Nancy Dwyer for assistance with the Zeiss LSM410 confocal microscope. We would also like to thank Brad Fletcher for helpful information and discussions concerning apoptosis and OGT. This work was supported by the Intramural Research Program of the National Institute of Diabetes and Digestive and Kidney Diseases in the National Institutes of Health.

Conflict of interest No human studies were involved in this manuscript. In addition, the authors declare that they have no conflict of interest.

Open Access This article is distributed under the terms of the Creative Commons Attribution Noncommercial License which permits any noncommercial use, distribution, and reproduction in any medium, provided the original author(s) and source are credited.

References

- Andrali SS, Marz P, Ozcan S (2005) Ataxin-10 interacts with *O*-GlcNAc transferase OGT in pancreatic beta cells. *Biochem Biophys Res Commun* 337:149–153
- Asfari M, Janjic D, Meda P, Li G, Halban PA, Wollheim CB (1992) Establishment of 2-mercaptoethanol-dependent differentiated insulin-secreting cell lines. *Endocrinology* 130:167–178
- Banerjee S, Robbins PW, Samuelson J (2009) Molecular characterization of nucleocytoplasmic *O*-GlcNAc transferases of *Giardia lamblia* and *Cryptosporidium parvum*. *Glycobiology* 19:331–336
- Boehmelt G, Wakeham A, Elia A, Sasaki T, Plyte S, Potter J, Yang Y, Tsang E, Ruland J, Iscove NN, Dennis JW, Mak TW (2000) Decreased UDP-GlcNAc levels abrogate proliferation control in EMeg32-deficient cells. *EMBO J* 19:5092–5104
- Brownlee M (2001) Biochemistry and molecular cell biology of diabetic complications. *Nature* 414:813–820
- Butkinaree C, Park K, Hart GW (2010) *O*-linked beta-*N*-acetylglucosamine (*O*-GlcNAc): extensive crosstalk with phosphorylation to regulate signaling and transcription in response to nutrients and stress. *Biochim Biophys Acta* 1800:96–106
- Champattanachai V, Marchase RB, Chatham JC (2007) Glucosamine protects neonatal cardiomyocytes from ischemia–reperfusion injury via increased protein-associated *O*-GlcNAc. *Am J Physiol Cell Physiol* 292:C178–C187
- Champattanachai V, Marchase RB, Chatham JC (2008) Glucosamine protects neonatal cardiomyocytes from ischemia–reperfusion injury via increased protein *O*-GlcNAc and increased mitochondrial Bcl-2. *Am J Physiol Cell Physiol* 294:C1509–C1520
- Chen D, Juarez S, Hartweck L, Alamillo JM, Simon-Mateo C, Perez JJ, Fernandez-Fernandez MR, Olszewski NE, Garcia JA (2005) Identification of secret agent as the *O*-GlcNAc transferase that participates in Plum pox virus infection. *J Virol* 79:9381–9387
- Filardo F, Robertson M, Singh DP, Parish RW, Swain SM (2009) Functional analysis of HvSPY, a negative regulator of GA response, in barley aleurone cells and *Arabidopsis*. *Planta* 229:523–537
- Fletcher BS, Dragstedt C, Notterpek L, Nolan GP (2002) Functional cloning of SPIN-2, a nuclear anti-apoptotic protein with roles in cell cycle progression. *Leukemia* 16:1507–1518
- Forsythe ME, Love DC, Lazarus BD, Kim EJ, Prinz WA, Ashwell G, Krause MW, Hanover JA (2006) *Caenorhabditis elegans* ortholog of a diabetes susceptibility locus: oga-1 (*O*-GlcNAcase) knockout impacts *O*-GlcNAc cycling, metabolism, and dauer. *Proc Natl Acad Sci USA* 103:11952–11957
- Fulop N, Marchase RB, Chatham JC (2007) Role of protein *O*-linked *N*-acetyl-glucosamine in mediating cell function and survival in the cardiovascular system. *Cardiovasc Res* 73:288–297
- Gambetta MC, Oktaba K, Muller J (2009) Essential role of the glycosyltransferase *sxc/Ogt* in polycomb repression. *Science* 325:93–96
- Hanover JA (2001) Glycan-dependent signaling: *O*-linked *N*-acetylglucosamine. *FASEB J* 15:1865–1876
- Hanover JA, Lai Z, Lee G, Lubas WA, Sato SM (1999) Elevated *O*-linked *N*-acetylglucosamine metabolism in pancreatic beta-cells. *Arch Biochem Biophys* 362:38–45
- Hanover JA, Yu S, Lubas WB, Shin SH, Ragano-Caracciola M, Kochran J, Love DC (2003) Mitochondrial and nucleocytoplasmic isoforms of *O*-linked GlcNAc transferase encoded by a single mammalian gene. *Arch Biochem Biophys* 409:287–297
- Hanover JA, Forsythe ME, Hennessey PT, Brodigan TM, Love DC, Ashwell G, Krause M (2005) A *Caenorhabditis elegans* model of insulin resistance: altered macronutrient storage and dauer formation in an OGT-1 knockout. *Proc Natl Acad Sci USA* 102:11266–11271
- Hanover JA, Krause MW, Love DC (2010) The hexosamine signaling pathway: *O*-GlcNAc cycling in feast or famine. *Biochim Biophys Acta* 1800:80–95
- Hart GW, Housley MP, Slawson C (2007) Cycling of *O*-linked beta-*N*-acetylglucosamine on nucleocytoplasmic proteins. *Nature* 446:1017–1022
- Hartweck LM, Scott CL, Olszewski NE (2002) Two *O*-linked *N*-acetylglucosamine transferase genes of *Arabidopsis thaliana* have overlapping functions necessary for gamete and seed development. *Genetics* 161:1279–1291
- Hartweck LM, Genger RK, Grey WM, Olszewski NE (2006) SECRET AGENT and SPINDLY have overlapping roles in the development of *Arabidopsis thaliana* L. Heyn. *J Exp Bot* 57:865–875
- Hu Y, Suarez J, Fricovsky E, Wang H, Scott BT, Trauger SA, Han W, Hu Y, Oyeleye MO, Dillmann WH (2009) Increased enzymatic *O*-GlcNAcylation of mitochondrial proteins impairs mitochondrial function in cardiac myocytes exposed to high glucose. *J Biol Chem* 284:547–555
- Kornfeld R (1967) Studies on L-glutamine D-fructose 6-phosphate amidotransferase. I. Feedback inhibition by uridine diphosphate-*N*-acetylglucosamine. *J Biol Chem* 242:3135–3141
- Kreppel LK, Hart GW (1999) Regulation of a cytosolic and nuclear *O*-GlcNAc transferase. Role of the tetratricopeptide repeats. *J Biol Chem* 274:32015–32022
- Kreppel LK, Blomberg MA, Hart GW (1997) Dynamic glycosylation of nuclear and cytosolic proteins. Cloning and characterization of a unique *O*-GlcNAc transferase with multiple tetratricopeptide repeats. *J Biol Chem* 272:9308–9315
- Laczy B, Hill BG, Wang K, Paterson AJ, White CR, Xing D, Chen YF, Darley-Usmar V, Oparil S, Chatham JC (2009) Protein *O*-GlcNAcylation: a new signaling paradigm for the cardiovascular system. *Am J Physiol Heart Circ Physiol* 296:H13–H28
- Lazarus BD, Love DC, Hanover JA (2006) Recombinant *O*-GlcNAc transferase isoforms: identification of *O*-GlcNAcase, yes

- tyrosine kinase, and tau as isoform-specific substrates. *Glycobiology* 16:415–421
- Lazarus BD, Love DC, Hanover JA (2009) *O*-GlcNAc cycling: implications for neurodegenerative disorders. *Int J Biochem Cell Biol* 41:2134–2146
- Liu K, Paterson AJ, Chin E, Kudlow JE (2000) Glucose stimulates protein modification by *O*-linked GlcNAc in pancreatic beta cells: linkage of *O*-linked GlcNAc to beta cell death. *Proc Natl Acad Sci USA* 97:2820–2825
- Liu K, Paterson AJ, Zhang F, McAndrew J, Fukuchi K, Wyss JM, Peng L, Hu Y, Kudlow JE (2004) Accumulation of protein *O*-GlcNAc modification inhibits proteasomes in the brain and coincides with neuronal apoptosis in brain areas with high *O*-GlcNAc metabolism. *J Neurochem* 89:1044–1055
- Love DC, Hanover JA (2005) The hexosamine signaling pathway: deciphering the “*O*-GlcNAc code”. *Sci STKE* 2005:re13
- Love DC, Kochan J, Cathey RL, Shin SH, Hanover JA (2003) Mitochondrial and nucleocytoplasmic targeting of *O*-linked GlcNAc transferases. *J Cell Sci* 116:647–654
- Love DC, Ghosh S, Mondoux MA, Fukushige T, Wang P, Wilson MA, Iser WB, Wolkow CA, Krause MW, Hanover JA (2010) *Proc Natl Acad Sci USA* 107:7413–7418
- Lubas WA, Hanover JA (2000) Functional expression of *O*-linked GlcNAc transferases. Domain structure and substrate specificity. *J Biol Chem* 275:10983–10988
- Lubas WA, Frank DW, Krause M, Hanover JA (1997) *O*-Linked GlcNAc transferase is a conserved nucleocytoplasmic protein containing tetratricopeptide repeats. *J Biol Chem* 272:9316–9324
- Marshall S, Bacote V, Traxinger RR (1991) Discovery of a metabolic pathway mediating glucose-induced desensitization of the glucose transport system. Role of hexosamine biosynthesis in the induction of insulin resistance. *J Biol Chem* 266:4706–4712
- Marz P, Stetefeld J, Bendfeldt K, Nitsch C, Reinstein J, Shoeman RL, Dimitriades-Schmutz B, Schwager M, Leiser D, Ozcan S, Otten U, Ozbek S (2006) Ataxin-10 interacts with *O*-linked beta-*N*-acetylglucosamine transferases in the brain. *J Biol Chem* 281:20263–20270
- McClain DA, Lubas WA, Cooksey RC, Hazel M, Parker GJ, Love DC, Hanover JA (2002) Altered glycan-dependent signaling induces insulin resistance and hyperleptinemia. *Proc Natl Acad Sci USA* 99:10695–10699
- Nakamura M, Barber AJ, Antonetti DA, LaNoue KF, Robinson KA, Buse MG, Gardner TW (2001) Excessive hexosamines block the neuroprotective effect of insulin and induce apoptosis in retinal neurons. *J Biol Chem* 276:43748–43755
- Olefsky JM (2001) Prospects for research in diabetes mellitus. *JAMA* 285:628–632
- Robertson M, Swain SM, Chandler PM, Olszewski NE (1998) Identification of a negative regulator of gibberellin action, HvSPY, in barley. *Plant Cell* 10:995–1007
- Roos MD, Hanover JA (2000) Structure of *O*-linked GlcNAc transferases: mediator of glycan-dependent signaling. *Biochem Biophys Res Commun* 271:275–280
- Roos MD, Xie W, Su K, Clark JA, Yang X, Chin E, Paterson AJ, Kudlow JE (1998) Streptozotocin, an analog of *N*-acetylglucosamine, blocks the removal of *O*-GlcNAc from intracellular proteins. *Proc Assoc Am Physicians* 110:422–432
- Shafi R, Iyer SP, Ellies LG, O'Donnell N, Marek KW, Chui D, Hart GW, Marth JD (2000) The *O*-GlcNAc transferase gene resides on the X chromosome and is essential for embryonic stem cell viability and mouse ontogeny. *Proc Natl Acad Sci USA* 97:5735–5739
- Silverstone AL, Tseng TS, Swain SM, Dill A, Jeong SY, Olszewski NE, Sun TP (2007) Functional analysis of SPINDLY in gibberellin signaling in Arabidopsis. *Plant Physiol* 143:987–1000
- Sinclair DA, Syrzycka M, Macauley MS, Rastgardani T, Komljenovic I, Vocado DJ, Brock HW, Honda BM (2009) *Drosophila O*-GlcNAc transferase (OGT) is encoded by the Polycomb group (PcG) gene, super sex combs (sxc). *Proc Natl Acad Sci USA* 106:13427–13432
- Slawson C, Housley MP, Hart GW (2006) *O*-GlcNAc cycling: how a single sugar post-translational modification is changing the way we think about signaling networks. *J Cell Biochem* 97:71–83
- Tang J, Neidigh JL, Cooksey RC, McClain DA (2000) Transgenic mice with increased hexosamine flux specifically targeted to beta-cells exhibit hyperinsulinemia and peripheral insulin resistance. *Diabetes* 49:1492–1499
- Vosseller K, Wells L, Lane MD, Hart GW (2002) Elevated nucleocytoplasmic glycosylation by *O*-GlcNAc results in insulin resistance associated with defects in Akt activation in 3T3-L1 adipocytes. *Proc Natl Acad Sci USA* 99:5313–5318
- Wells L, Vosseller K, Hart GW (2001) Glycosylation of nucleocytoplasmic proteins: signal transduction and *O*-GlcNAc. *Science* 291:2376–2378
- Wu T, Zhou H, Jin Z, Bi S, Yang X, Yi D, Liu W (2009) Cardioprotection of salidroside from ischemia/reperfusion injury by increasing *N*-acetylglucosamine linkage to cellular proteins. *Eur J Pharmacol* 613:93–99